Transport in superconducting wires

Junaid Majeed Bhat and Abhishek Dhar

International Centre for Theoretical Sciences, Tata Institute of Fundamental Research, Bengaluru-560089, India

(Dated: August 3, 2022)

We consider electron transport in a model of a spinless superconductor described by a Kitaev type lattice Hamiltonian where the electron interactions are modelled through a superconducting pairing term. The superconductor is sandwiched between two normal metals kept at different temperatures and chemical potentials and are themselves modelled as non-interacting spinless fermions. For this set-up we compute the exact steady state properties of the system using the quantum Langevin equation approach. The closed form exact expressions for current and other two-point correlations are obtained in the Landauer-type forms and involve two nonequilibrium Green's functions. We then discuss a numerical approach where we construct the time-evolution of the two point correlators of the system from the eigenspectrum of the complete quadratic Hamiltonian describing the system and leads. By starting from an initial state corresponding to the leads in thermal equilibrium and the system in an arbitrary state, the long time solution for the correlations, before recurrence times, gives us steady state properties. We use this independent numerical method for verifying the results of the exact solution and to comment on the role of bound states. Our results are quite general and applicable to arbitrary lattices in any dimensions.

I. INTRODUCTION

The Kitaev chain models a one-dimensional spinless p-wave superconductor[1] and provides one of the simplest examples of a topological insulator. This system has the so-called Majorana Bound States (MBS), which are topologically protected zero-energy bound states, localised at the boundaries of an open chain. Several proposals were put forward[2–6] to realise the Kitaev chain experimentally and observe the MBS. Some of these experimental proposals have already been successfully implemented[7–12]. One of the key experimental signatures of the MBS is the zero-bias peak in the differential tunnelling conductance and this has been seen in experiments[7–9]. However, these experiments show several deviations from the expected theoretical results. For example, the strength of the zero-bias peak was found to be much smaller than the expected value $2e^2/h$. A comprehensive discussion of some of the issues can be found in Ref. [13]. A complete understanding of the transport properties of such superconducting wires and topological wires is still lacking. Kitaev's model is one of the simplest physical model for realising MBS. Its transport properties would thereby play a crucial role in understanding the special role of MBS.

We note that many of the interesting topological characteristics can be understood in the context of the isolated system, in either the geometry with free boundary conditions or one with periodic boundary conditions. One can also extract interesting results on transport within the framework of the Green-Kubo formalism[14]. However experiments on transport are typically done with leads and reservoirs, kept at different chemical potentials and temperatures, and understanding this requires the framework of open quantum systems. One could expect that the MBS at the ends of a Kitaev chain would get affected on coupling the wire to infinite leads (made of normal material). Some of the open system approaches that have been used to understand transport in superconducting wires include scattering approach[15–17], nonequilibrium Keldysh Green's function (NEGF) approach[13,18,19] and the quantum Langevin equation approach[20]. One of the earliest study of electron transport through superconducting channels was by Blonder, Tinkham, and Klapwijk[15]. In their approach, the electron transport properties of a superconducting channel were studied by considering scattering of a plane wave at a junction separating normal metal and the superconductor(NS junction) and the important role of Andreev reflection was pointed out. A similar approach has been used in Ref. [16] to study conductance of a one-dimensional system consisting of a p-wave superconductor connected to leads at the two ends (NSN junction). Another numerical approach that has been used to study transport in superconducting wires connected to normal wires uses the fact that the models involve quadratic Hamiltonians and hence a direct diagonalization is possible for quite long chains. In a recent work[21], this approach was used to study transport in various configurations of normal and superconducting wires and it was noted that bound states could lead to persistent oscillating currents in the system.

The quantum Langevin equations (QLE) approach[22] provides one of the most direct and intuitive approaches for open quantum systems. Here one writes the effective dynamics of a system coupled to thermal and particle reservoirs, and this can be used to obtain the NEGF results, for both electronic and phononic systems[23,24]. The nonequilibrium transport properties of the Kitaev chain were first studied using the QLE-NEGF formalism in Ref. [20] and several interesting results were obtained. In particular, the variation of differential conductance with the wire length and the current voltage characteristics of the wire were studied.

In the present work we extend the analysis in Ref. [20] to obtain the nonequilibrium steady state (NESS) prop-

erties of a spinless superconductor defined on an arbitrary lattice in any dimension, the Kitaev chain occurs as a special case. Using the QLE-NEGF formalism, we obtain exact formal expressions for the current, density and other two-point correlations in terms of nonequilibrium Green's functions. In particular we find that all quantities can be expressed in terms of a pair of retarded and advanced Green's functions $G_1^\pm(\omega)$ and $G_2^\pm(\omega)$. Secondly, noting that the system is described by a quadratic Hamiltonian, we use an exact numerical scheme to study the microscopic time evolution of the coupled system and reservoirs, starting from a product initial condition. Using this numerical scheme for the Kitaev chain, we verify the analytic results from the QLE-NEGF formalism, for chains of finite lengths. We comment on various issues that arise in parameter regimes where the combined system-reservoirs has bound states.

This paper is structured as follows. In Sec. (II), we define the precise model of a spinless superconductor (which we refer to as the Kitaev wire) coupled to two thermal reservoirs made of free fermions. Starting from the Heisenberg equations of motion, we obtain the effective quantum Langevin equations for the wire. In Sec. (III), these Langevin equations of motion are solved using Fourier transform to get the steady state solution for the current and two-point correlations in the wire. In Sec. (IV), we present a different formal method to compute two-point correlators at all times using the exact diagonalization of the quadratic Hamiltonian describing the superconductor. In particular this gives us the current and the densities at any finite time. For finite systems, this method is numerically implemented in Sec. (V), for the special case of a one-dimensional Kitaev chain (connected to normal baths) and a comparison is made with the steady state results obtained using the methods of Sec. (II). We conclude with a discussion in Sec. (VI).

II. QUANTUM LANGEVIN EQUATIONS AND GREEN'S FUNCTION FORMALISM

We consider a wire coupled to thermal baths on its two ends. The wire Hamiltonian, $\mathcal{H}^W$, is taken to correspond to a spinless superconductor while the two baths are modelled by the tight binding Hamiltonians, $\mathcal{H}^L$ and $\mathcal{H}^R$. The L and R superscripts denote the baths on the left and the right of the wire respectively. The couplings of the wire with the two baths, $\mathcal{H}^{WR}$ and $\mathcal{H}^{WL}$, are also modelled by tight binding Hamiltonians. Let us denote by $\{c_m, c_m^\dagger\}$, $\{c_\nu, c_\nu^\dagger\}$ and $\{c_{\nu'}, c_{\nu'}^\dagger\}$ the annihilation and creation operators of the system, left bath and the right bath respectively. These satisfy usual fermionic anticommutation relations. For lattice sites on the bath we use the Latin indices, $i, j, ...$, for sites on the left reservoir we use the Greek indices, $\alpha, \nu, ...$, and for sites on the right reservoir, the primed Greek letters $\alpha', \nu', ...$ We take the Hamiltonian of the full system of wire and baths

as follows:

$$\mathcal{H} = \mathcal{H}^W + \mathcal{H}^{WL} + \mathcal{H}^{WR} + \mathcal{H}^L + \mathcal{H}^R, \quad (1)$$

where

$$\mathcal{H}^W = \sum_{mn} H_{mn}^W c_m^\dagger c_n + \Delta_{mn} c_m^\dagger c_n^\dagger + \Delta_{mn}^\dagger c_m c_n, \quad (2)$$

$$\mathcal{H}^{WL} = \sum_{\nu m} V_{m\nu}^L c_m^\dagger c_\nu + V_{\nu m}^{L\dagger} c_\nu^\dagger c_m, \quad (3)$$

$$\mathcal{H}^{WR} = \sum_{\nu' m} V_{m\nu'}^R c_m^\dagger c_{\nu'} + V_{\nu' m}^{R\dagger} c_{\nu'}^\dagger c_m, \quad (4)$$

$$\mathcal{H}^L = \sum_{\mu\nu} H_{\mu\nu}^L c_\mu^\dagger c_\nu, \quad (5)$$

$$\mathcal{H}^R = \sum_{\mu'\nu'} H_{\mu'\nu'}^R c_{\mu'}^\dagger c_{\nu'}. \quad (6)$$

The model considered here is quite general in the sense that we allow non-zero hopping elements between arbitrary sites and similarly the superconducting pairing term is allowed between any pair of sites. Thus there are no restrictions on dimensionality and the structure of the underlying lattice and the range of the interactions. The results for the one-dimensional Kitaev chain with nearest neighbour interactions follows as a special case.

We now follow the approach of Ref. [23] to obtain the NEGF-type results for this system. First we note that the Heisenberg equations of motion for the wire sites and bath sites are given by:

$$\dot{c}_l = -i \sum_m H_{lm}^W c_m - i \sum_m K_{lm} c_m^\dagger$$
$$\qquad - i \sum_\alpha V_{l\alpha}^L c_\alpha - i \sum_{\alpha'} V_{l\alpha'}^R c_{\alpha'}, \quad (7)$$

$$\dot{c}_\alpha = -i \sum_\nu H_{\alpha\nu}^L c_\nu - i \sum_l V_{\alpha l}^{L\dagger} c_l, \quad (8)$$

$$\dot{c}_{\alpha'} = -i \sum_{\nu'} H_{\alpha'\nu'}^R c_\nu - i \sum_l V_{\alpha' l}^{R\dagger} c_l, \quad (9)$$

where $K_{lm} = (\Delta - \Delta^T)_{lm}$. We treat the term containing c_l in Eq. (8) and Eq. (9) as the inhomogeneous parts and solve these equations using the following Green's functions corresponding to the homogeneous part of the equations:

$$g_L^+(t) = -i e^{-itH^L} \theta(t) = \int_{-\infty}^\infty \frac{d\omega}{2\pi} g_L^+(\omega) e^{-i\omega t}, \quad (10)$$

$$g_R^+(t) = -i e^{-itH^R} \theta(t) = \int_{-\infty}^\infty \frac{d\omega}{2\pi} g_R^+(\omega) e^{-i\omega t}. \quad (11)$$

In terms of these, we obtain the following solutions for

the reservoir equations (for $t > t_0$):

$$c_\alpha(t) = i \sum_\nu [g_L^+(t - t_0)]_{\alpha\nu} c_\nu(t_0)$$
$$+ \int_{t_0}^t ds \sum_{\nu l} [g_L^+(t - s)]_{\alpha\nu} V_{\nu l}^{L\dagger} c_l(s), \tag{12}$$

$$c_{\alpha'}(t) = i \sum_{\nu'} [g_R^+(t - t_0)]_{\alpha'\nu'} c_{\nu'}(t_0)$$
$$+ \int_{t_0}^t ds \sum_{\nu' l} [g_R^+(t - s)]_{\alpha'\nu'} V_{\nu' l}^{R\dagger} c_l(s). \tag{13}$$

Substituting these results in the Heisenberg equation for the wire sites we have:

$$\dot{c}_l = -i \sum_m H_{lm}^W c_m - i \sum_m K_{lm} c_m^\dagger - i\eta_l^L - i\eta_l^R$$
$$- i \int_{t_0}^t ds \sum_{\alpha\nu m} V_{l\alpha}^L [g_L^+(t - s)]_{\alpha\nu} V_{\nu m}^{L\dagger} c_m(s)$$
$$- i \int_{t_0}^t ds \sum_{\alpha'\nu' m} V_{l\alpha'}^R [g_R^+(t - s)]_{\alpha'\nu'} V_{\nu' m}^{R\dagger} c_m(s), \tag{14}$$

where

$$\eta_l^L = i \sum_{\alpha\nu} V_{l\alpha}^L [g_L^+(t - t_0)]_{\alpha\nu} c_\nu(t_0), \tag{15}$$

$$\eta_l^R = i \sum_{\alpha'\nu'} V_{l\alpha'}^R [g_L^+(t - t_0)]_{\alpha'\nu'} c_{\nu'}(t_0). \tag{16}$$

At $t = t_0$, we choose the two reservoirs to be described by grand canonical ensembles at temperatures and chemical potentials given by (T_L, μ_L) and (T_R, μ_R) respectively. This allows us to determine the correlation properties of the terms η_l^L and η_l^R. For the left bath we have:

$$\langle \eta_l^L(t)\eta_m^L(t')\rangle = \langle \eta_l^{L\dagger}(t)\eta_m^{L\dagger}(t')\rangle = 0, \tag{17}$$

$$\langle \eta_l^{L\dagger}(t)\eta_m^L(t')\rangle = \sum_{\alpha\mu\nu\sigma} V_{l\alpha}^{L*} [g_L^{+*}(t - t_0)]_{\alpha\nu} V_{m\mu}^L$$
$$[g_L^+(t' - t_0)]_{\mu\sigma} \langle c_\nu^\dagger(t_0)c_\sigma(t_0)\rangle, \tag{18}$$

with similar expressions for η_l^R. We thus see that Eq. (14) has the structure of a quantum Langevin equation for the wire where the reservoir contributions are split into noise (terms given by η_l^L and η_l^R), and dissipation (the terms in Eq. (14) involving integral kernels).

At this point we take a digression to simplify Eq. (18) and write it in Fourier space. Let $\psi_q^L(\alpha)$ and λ_q^L be the single-particle eigenvectors and eigenvalues of the left reservoir Hamiltonian, $\mathcal{H}^L$. Using this and the fact that the left bath is initially described by a grand canonical

ensemble with temperature T_L and chemical potential μ_L we get

$$[g_L^+(t - t_0)]_{\nu\sigma} = -i\theta(t - t_0) \sum_q \psi_q^L(\nu)\psi_q^{L*}(\sigma)e^{-i\lambda_q^L(t-t_0)}, \tag{19}$$

$$\langle c_\nu^\dagger(t_0)c_\sigma(t_0)\rangle = \sum_q \psi_q^{L*}(\nu)\psi_q^L(\sigma)f_L(\lambda_q^L), \tag{20}$$

where $f_L(\lambda_q^L) = f(\lambda_q^L, \mu_L, T_L)$ is the Fermi-Dirac distribution function. Using these two equations in Eq. (18) we have:

$$\langle \eta_l^{L\dagger}(t)\eta_m^L(t')\rangle$$
$$= \sum_{\alpha\nu} V_{l\alpha}^{L*} \left(\sum_q \psi_q^{L*}(\alpha)\psi_q^L(\nu)e^{i\lambda_q^L(t-t')}f_L(\lambda_q^L) \right) V_{\nu m}^{LT}. \tag{21}$$

Defining the Fourier transform

$$\tilde{\eta}_l(\omega) = \int_{-\infty}^\infty \frac{dt}{2\pi}\eta_l(t)e^{i\omega t}, \tag{22}$$

we finally get the Fourier transform form of Eq. (21) as:

$$\langle \tilde{\eta}_l^{L\dagger}(\omega)\tilde{\eta}_m^L(\omega')\rangle = \Gamma_{ml}^L(\omega)f_L(\omega)\delta(\omega - \omega'), \tag{23}$$

where $\Gamma_{ml}^L(\omega) = (V^L\rho^L V^{L\dagger})_{ml}$ and $\rho_{\alpha\nu}^L = \sum_q \psi_q^L(\alpha)\psi_q^{L*}(\nu)\delta(\omega - \lambda_q^L)$. Using Eq. (23) we can also show that

$$\langle \tilde{\eta}_l^L(\omega)\tilde{\eta}_m^{L\dagger}(\omega')\rangle = \Gamma_{lm}^L(\omega) [1 - f_L(\omega)] \delta(\omega - \omega'). \tag{24}$$

The correlation properties of the right bath would be of the same form.

Let us now return back to Eq. (14) and obtain its steady state solution. For this we assume that one has taken the limits of infinite bath degrees of freedom and the time $t_0 \to -\infty$. Then it is expected that a steady state should exist provided certain conditions are satisfied[23]. For now we assume the existence of a steady state and will re-visit this question in the next section. The Langevin equation in Eq. (14) is then amenable to a solution by Fourier transforms. To this end, we define

$$\tilde{c}_l(\omega) = \int_{-\infty}^\infty \frac{dt}{2\pi}c_l(t)e^{i\omega t}, \tag{25}$$

and substitute this in Eq. (14) to get

$$[\Pi(\omega)]_{lm}\tilde{c}_m(\omega) - K_{lm}\tilde{c}_m^\dagger(-\omega) = \tilde{\eta}_l^L(\omega) + \tilde{\eta}_l^R(\omega), \tag{26}$$

where

$$\Pi(\omega) = \omega - H^W - \Sigma_L^+(\omega) - \Sigma_R^+(\omega), \tag{27}$$

$$\Sigma_L^+(\omega) = V^L g_L^+(\omega)V^{L\dagger}, \quad \Sigma_R^+(\omega) = V^R g_R^+(\omega)V^{R\dagger}. \tag{28}$$

With some algebra one can also show:

$$\Gamma_L(\omega) = \frac{1}{2\pi i}\big[\Sigma_L^-(\omega) - \Sigma_L^+(\omega)\big], \qquad (29)$$

$$\Gamma_R(\omega) = \frac{1}{2\pi i}\big[\Sigma_R^-(\omega) - \Sigma_R^+(\omega)\big], \qquad (30)$$

where $\Sigma_L^- = [\Sigma_L^+]^\dagger$ and $\Sigma_R^- = [\Sigma_R^+]^\dagger$. We now write Eq. (26) in matrix form as:

$$\Pi(\omega)\tilde{C}(\omega) - K\tilde{C}^\dagger(-\omega) = \tilde{\eta}^L(\omega) + \tilde{\eta}^R(\omega), \qquad (31)$$

where $\tilde{C}(\omega)$, $\tilde{C}^\dagger(\omega)$ and $\tilde{\eta}^{L/R}(\omega)$ are column matrices with components $\tilde{c}_m(\omega)$, $\tilde{c}_m^\dagger(\omega)$ and $\tilde{\eta}_l^{L/R}(\omega)$ respectively. A complex conjugation of Eq. (26) and transforming $\omega \to -\omega$ gives us the following matrix equation:

$$\Pi^*(-\omega)\tilde{C}^\dagger(-\omega) - K^*\tilde{C}(\omega) = \eta^{L\dagger}(-\omega) + \eta^{R\dagger}(-\omega) \quad (32)$$

Using Eq. (32) and Eq. (31) we finally obtain the following expression for $\tilde{c}_m(\omega)$:

$$\tilde{c}_m(\omega) = [G_1^+(\omega)]_{ml}\big[\tilde{\eta}_l^L(\omega) + \tilde{\eta}_l^R(\omega)\big]$$
$$+ [G_2^+(\omega)]_{ml}\big[\tilde{\eta}_l^{L\dagger}(-\omega) + \tilde{\eta}_l^{R\dagger}(-\omega)\big], \qquad (33)$$

where

$$G_1^+(\omega) = \frac{1}{\Pi(\omega) + K[\Pi^*(-\omega)]^{-1}K^\dagger}, \qquad (34)$$

$$G_2^+(\omega) = G_1^+(\omega)K[\Pi^*(-\omega)]^{-1}. \qquad (35)$$

Thus we have obtained the steady state solution in terms of these two nonequilibrium Green's functions.

III. NONEQUILIBRIUM STEADY STATE PROPERTIES

Using the solution for $\tilde{c}_m(\omega)$ and the noise properties obtained in the previous section, we now proceed to compute expectation values of various physical observables which are along quadratic functions of the fermionic operators.

A. Steady state current

We first define the particle current in the wire. Clearly, the rate of change of total number of particles in the left bath, $N_L = \sum_\alpha c_\alpha^\dagger c_\alpha$, gives the particle current, J_L, entering the wire from the left reservoir. A straightforward calculation then gives

$$J_L = 2\sum_{m\alpha} \text{Im}[V_{m\alpha}^L \langle c_m^\dagger(t)c_\alpha(t)\rangle] \qquad (36)$$

$$= 2\,\text{Im}\Bigg[\sum_m \int_{-\infty}^\infty \int_{-\infty}^\infty d\omega d\omega' e^{i(\omega-\omega')t}$$
$$\Big\langle c_m^\dagger(\omega)\sum_\alpha V_{m\alpha}^L c_\alpha(\omega')\Big\rangle\Bigg] \qquad (37)$$

From the Fourier transform of Eq. (8) we have

$$\sum_\alpha V_{m\alpha}^L \tilde{c}_\alpha(\omega') = \eta_m^L(\omega') + [\Sigma_L^+(\omega')]_{ml}\tilde{c}_l(\omega'). \qquad (38)$$

Using Eqs. (29,30,33) and the correlation properties of the noise terms we finally obtain the following expression for current:

$$\frac{J_L}{2\pi} =$$
$$\int_{-\infty}^\infty d\omega\bigg(\text{Tr}\big[G_1^+(\omega)\Gamma_R(\omega)G_1^-(\omega)\Gamma_L(\omega)\big](f_L(\omega) - f_R(\omega))$$
$$+ \text{Tr}\big[G_2^+(\omega)\Gamma_R^T(-\omega)G_2^-(\omega)\Gamma_L(\omega)\big](f_R(-\omega) + f_L(\omega) - 1)$$
$$+ \text{Tr}\big[G_2^+(\omega)\Gamma_L^T(-\omega)G_2^-(\omega)\Gamma_L(\omega)\big](f_L(-\omega) + f_L(\omega) - 1)\bigg),$$
$$(39)$$

where $G_1^-(\omega) = [G_1^+(\omega)]^\dagger$, $G_2^-(\omega) = [G_2^+(\omega)]^\dagger$, $f_L(\omega) = f(\omega, \mu_L, T_L)$ and $f_R(\omega) = f(\omega, \mu_R, T_R)$. This general NEGF-type expression for the particle current is one of our main results. The details of the calculation are presented in the appendix. A similar expression can be obtained for J_R which we define as the current from the right reservoir into the system.

For $\Delta = 0$ case, it is straightforward to see that Eq. (39) agrees with the expression for the current obtained in Ref. [23]. Also, for $\mu_L = -\mu_R = \mu$ and $T_L = T_R = T$ it reduces to

$$\frac{J_L}{2\pi} = \int_{-\infty}^\infty d\omega \mathcal{A}_L(\omega)(f(\omega, \mu, T) - f(\omega, -\mu, T)),$$

where $\mathcal{A}_L(\omega) = \text{Tr}\big[G_1^+(\omega)\Gamma_R(\omega)G_1^-(\omega)\Gamma_L(\omega)\big] + \text{Tr}\big[G_2^+(\omega)\Gamma_L^T(-\omega)G_2^-(\omega)\Gamma_L(\omega)\big]$. This form agrees with the current expression derived in Ref. [20] for a Kitaev chain with nearest neighbour interactions.

From Eq. (39) we see that for $T_L = T_R, \mu_L = \mu_R$, $J_L, J_R \neq 0$ whenever $\Delta \neq 0$ and, in general, the current at the left end and the right end are different, i.e $J_L \neq -J_R$. This result initially appears to be surprising, but is basically due to the fact that the superconducting pairing matrix Δ_{lm} in the Kitaev wire is not calculated self-consistently but is taken as a fixed parameter of the wire Hamiltonian. This becomes clear if we consider the equation for the total number operator of the wire:

$$\frac{\mathrm{d}}{\mathrm{d}t}\bigg(\sum_l \langle c_l^\dagger(t)c_l(t)\rangle\bigg) = J_S + J_L + J_R, \qquad (40)$$

where $J_S = \sum_{l,m} 2\,\text{Im}\big\{K_{lm}\langle c_l^\dagger c_m^\dagger\rangle\big\}$ is the extra contribution from the superconducting terms of the wire Hamiltonian. In the steady state the left hand side vanishes and the fact that $J_L + J_R \neq 0$ can be understood in terms of the extra pairing current J_S. Physically our set-up corresponds to a wire that is in contact with a superconducting wire and the so-called proximity effect

induces superconductivity in the wire. The superconducting substrate acts as an electron reservoir[13,18,25] and acts like a ground for the wire. Thus current can enter the wire through the left and right reservoirs and flow into the superconductor. Also, J_S need not vanish even when the baths are initially at the same chemical potentials and temperatures and hence, J_L and J_R may take non-zero values. Note that imposing the self-consistency condition, namely

$$K_{lm} = \langle c_m c_l \rangle = \langle c_l^\dagger c_m^\dagger \rangle^*, \tag{41}$$

for all l, m, would give $J_S = 0$ and in that case we would get the expected charge conservation condition $J_L = -J_R$.

B. Two point correlations

We now compute the full two-point correlation matrices $\langle c_l^\dagger c_m \rangle$, $\langle c_l c_m \rangle$, $\langle c_l^\dagger c_m^\dagger \rangle$ in the NESS. These would allow one to obtain the local particle densities, $\langle c_l^\dagger c_l \rangle$, and local currents (normal and superconducting) anywhere in the system. We start by writing the correlations in the Fourier representation:

$$\langle c_m^\dagger(t)c_n(t) \rangle = \int \int d\omega d\omega' e^{i(\omega'-\omega)t} \langle c_m^\dagger(\omega)c_n(\omega') \rangle. \tag{42}$$

Then using the solution in Eq. (33) and the noise properties a straightforward computation gives:

$$\langle c_m^\dagger(t)c_n(t) \rangle = \int d\omega [G_1^+(\omega)\Gamma_L(\omega)G_1^-(\omega)]_{nm} f_L(\omega)$$
$$+ [G_2^+(\omega)\Gamma_L^T(-\omega)G_2^-(\omega)]_{nm} [1 - f_L(-\omega)]$$
$$+ \int d\omega [G_1^+(\omega)\Gamma_R(\omega)G_1^-(\omega)]_{nm} f_R(\omega)$$
$$+ [G_2^+(\omega)\Gamma_R^T(-\omega)G_2^-(\omega)]_{nm} [1 - f_R(-\omega)]. \tag{43}$$

A similar computation gives

$$\langle c_i(t)c_j(t) \rangle = \int d\omega [Q_L(\omega)]_{ij} + [Q_L^T(\omega) - Q_L(\omega)]_{ij} f_L(\omega)$$
$$+ \int d\omega [Q_R(\omega)]_{ij} + [Q_R^T(\omega) - Q_R(\omega)]_{ij} f_R(\omega), \tag{44}$$

where $Q_{L/R}(\omega) = G_1^+(\omega)\Gamma_{L/R}(\omega)G_2^{+T}(-\omega)$. Substituting this in the expression for $J_S = \sum_{l,m} 2 \operatorname{Im}\{K_{lm}\langle c_l^\dagger c_m^\dagger \rangle\}$, we get its steady state value,

$$J_S = 2 \int d\omega \operatorname{Im}\{\operatorname{Tr}[Q_L^\dagger(\omega)K]\}(2f_L(\omega) - 1)$$
$$+ \operatorname{Im}\{\operatorname{Tr}[Q_R^\dagger(\omega)K]\}(2f_R(\omega) - 1) \tag{45}$$

From Eq. (44), it also follows that $\langle \{c_i(t), c_j(t)\} \rangle = \int d\omega [Q_L(\omega) + Q_L^T(\omega) + Q_R(\omega) + Q_R^T(\omega)]_{ij} = I_{ij}$. It

turns out that these integrals do not always vanish. This is at first surprising since we expect that the usual anti-commutation properties of the fermionic operators should hold. The underlying reason is that the results presented so far assume the existence of a steady state. However this is true only if there are no bound states in the system (wire+baths). In case there are bound states present in the system, then their contributions to the expressions of the correlations have to be added separately. For the case of Eq. (44), the contribution from the bound state would ensure the vanishing of $\langle \{c_i(t), c_j(t)\} \rangle$. In the next section we will demonstrate this explicitly via numerics for the one dimensional Kitaev chain and show that for parameter regimes with no bound states, the integrals I_{ij} do vanish. This does not appear straightforward to show analytically because for the Hamiltonian in Eq. (1), it is somewhat non-trivial to find the parameter regimes for bound states to be absent. Note that the conditions for bound states (MBS) in the isolated Kitaev chain will not be the same as those for the chain connected to non-superconducting reservoirs.

IV. AN EXACT NUMERICAL APPROACH FOR COMPUTING CORRELATIONS IN FINITE SYSTEMS

The fact that our system is described by a quadratic Hamiltonian means that the exact diagonalization of the system becomes a much simpler problem[21,26]. Let N_S be the total number of lattice sites in the entire system of wire and the two reservoirs. Then instead of diagonalizing a $2^{N_S} \times 2^{N_S}$ matrix, the problem reduces to the diagonalization of a $2N_S \times 2N_S$ matrix. To see this we define a $2N_S$-component column vector:

$$\chi = \begin{pmatrix} C \\ C^\dagger \end{pmatrix}, \text{where } C = \begin{pmatrix} C_W \\ C_L \\ C_R \end{pmatrix}, \tag{46}$$

and C_W, C_L and C_R are column vectors containing the wire, left bath and the right bath operators respectively. Note that $\chi_{N_S+i}^\dagger = \chi_i$, for $i = 1, 2, \ldots, N_S$. We can then write the Hamiltonian in Eq. (1) in the form

$$\mathcal{H} = \frac{1}{2}\chi^\dagger \mathcal{Z}\chi + \frac{1}{2}\operatorname{Tr}[H_S], \tag{47}$$

where $\mathcal{Z}$ is a $2N_S \times 2N_S$ matrix defined as

$$\mathcal{Z} = \begin{pmatrix} H_S & K_S \\ K_S^\dagger & -H_S^* \end{pmatrix}, \tag{48}$$

with

$$H_S = \begin{pmatrix} H_W & V_L & V_R \\ V_L^\dagger & H_L & 0 \\ V_R^\dagger & 0 & H_R \end{pmatrix} \text{ and } K_S = \begin{pmatrix} K & 0 & 0 \\ 0 & 0 & 0 \\ 0 & 0 & 0 \end{pmatrix}. \tag{49}$$

As can be easily verified, the $2N_S$ eigenvectors of the matrix $\mathcal{Z}$ occur in pairs of the form

$$
\Psi_i = \begin{pmatrix} u_1(i) \\ u_2(i) \\ . \\ . \\ u_{N_S}(i) \\ v_1(i) \\ . \\ . \\ v_{N_S}(i) \end{pmatrix} \quad \Phi_i = \begin{pmatrix} v_1^*(i) \\ v_2^*(i) \\ . \\ . \\ v_{N_S}^*(i) \\ u_1^*(i) \\ . \\ . \\ u_{N_S}^*(i) \end{pmatrix}, \quad i = 1, 2, \ldots, N_S,
$$

(50)

where the eigenvectors Ψ_i and Φ_i correspond respectively to eigenvalues ϵ_i and $-\epsilon_i$. Let us define the $N_S \times N_S$ matrices U, V and E with matrix elements $U_{si} = u_s(i)$, $V_{si} = v_s(i)$ and $E_{ij} = \epsilon_i \delta_{ij}$, respectively. Then we see that the matrix W which diagonalizes $\mathcal{Z}$ has the structure

$$
W = \begin{pmatrix} U & V^* \\ V & U^* \end{pmatrix}, \tag{51}
$$

so that

$$
W^\dagger Z W = \begin{pmatrix} E & 0 \\ 0 & -E \end{pmatrix}. \tag{52}
$$

We define new fermionic variables $\zeta = W^\dagger \chi$ and note that due to the structure in Eq. (51), $\zeta_{N_S+i} = \zeta_i^\dagger$, for $i = 1, 2, \ldots, N_S$. Note that this transformation mixes the operators corresponding to different sites of the wire and the bath, and the index i does not refer to any lattice site. The ζ_i correspond to the "normal modes" of the system. In this basis the Hamiltonian then takes the form

$$
\mathcal{H} = \sum_{i=1}^{N_S} \epsilon_i \left(\zeta_i^\dagger(t) \zeta_i(t) - \frac{1}{2} \right) + \frac{1}{2} \operatorname{Tr}[H_S]. \tag{53}
$$

The evolution of the ζ operators is simply given by $\zeta_j(t) = e^{-i\epsilon_j t} \zeta_j(0)$. Therefore, a two point correlator of the original operators at any time t can be expressed in terms of ζ operators at $t = 0$ via the transformation W. For the correlator $\langle c_p^\dagger(t) c_q(t) \rangle$, where p, q denotes any site on the entire system, we thus obtain:

$$
\langle c_p^\dagger(t) c_q(t) \rangle = \sum_{l,m=1}^{N_S} \left[\mathcal{T}_{N_S+p,q}^{N_S+l,N_S+m} e^{i(\epsilon_l+\epsilon_m)t} \langle \zeta_l^\dagger \zeta_m^\dagger \rangle \right.
$$
$$
+ \mathcal{T}_{N_S+p,q}^{lm} e^{-i(\epsilon_l+\epsilon_m)t} \langle \zeta_l \zeta_m \rangle + \mathcal{T}_{N_S+p,q}^{N_S+l,m} e^{-i(-\epsilon_l+\epsilon_m)t} \langle \zeta_l^\dagger \zeta_m \rangle
$$
$$
\left. + \mathcal{T}_{N_S+p,q}^{l,N_S+m} e^{-i(\epsilon_l-\epsilon_m)t} \langle \zeta_l \zeta_m^\dagger \rangle \right], \tag{54}
$$

where $\mathcal{T}_{pq}^{lm} = W_{pl} W_{qm}$ and ζ_i in the above equation denotes $\zeta_i(0)$. Using the transformation $\zeta = W^\dagger \chi$, the two point correlations of the ζ operators at $t = 0$ can be determined from the two point correlations of c_p and $c_p^\dagger$ at $t = 0$, which are known once the initial state of the system is specified. In particular we know these correlations

for the product initial state used in the previous section, where the reservoirs are described by thermal states with specified temperatures and chemical potentials, while the system is in an arbitrary initial state.

The numerical approach thus consists of finding the eigenspectrum of the matrix $\mathcal{Z}$ and then computing the time evolution of any two-point correlator using Eq. (54). Our interest will be in looking at correlations in the wire. For a finite bath we expect to see steady state behaviour of the wire correlations in a time window, which is after some initial transients and before the finite bath effects show up. Thus the correlations would first show some initial evolution, then show a long plateau before finite size effects show up. The steady state properties can be extracted from the plateau region We will now use this procedure to directly verify the steady state results given by the analytic expressions in the previous section. We will also look for the existence of bound states in the spectrum of the matrix $\mathcal{Z}$ and explore their effect on the steady state. The bound state energy would lie outside the band width of the baths and the corresponding eigenvector would be spatially localized.

V. NUMERICAL VERIFICATION OF QLE-NEGF RESULTS

We apply the numerical approach of the previous section on the one-dimensional Kitaev chain to verify the analytical results in Sec. (III). We consider a one-dimensional system with N sites on the wire and N_b on each of the two baths and so $N_S = N + 2N_b$. The full system Hamiltonian is given by:

$$
\mathcal{H} = \mathcal{H}_W + \mathcal{H}_L + \mathcal{H}_{WL} + \mathcal{H}_R + \mathcal{H}_{WR}
$$
$$
= \sum_{j=1}^{N-1} \left[-\eta_s(a_j^\dagger a_{j+1} + a_{j+1}^\dagger a_j) + \Delta(a_j a_{j+1} + a_{j+1}^\dagger a_j^\dagger) \right]
$$
$$
+ \sum_{\alpha=1}^{N_b-1} \left[-\eta_b(b_\alpha^{L\dagger} b_{\alpha+1}^L + b_{\alpha+1}^{L\dagger} b_\alpha^L) \right] - V_L(a_1^\dagger b_1^L + b_1^{L\dagger} a_1)
$$
$$
+ \sum_{\alpha'=1}^{N_b-1} \left[-\eta_b(b_{\alpha'}^{R\dagger} b_{\alpha'+1}^R + b_{\alpha'+1}^{R\dagger} b_{\alpha'}^R) \right] - V_R(a_N^\dagger b_1^R + b_1^{R\dagger} a_N),
$$

(55)

where $\{a_j, a_j^\dagger\}$, $\{b_\alpha^R, b_\alpha^{R\dagger}\}$, $\{b_{\alpha'}^L, b_{\alpha'}^{L\dagger}\}$ are creation and annihilation operators on the wire, right and left bath sites respectively. As in Sec. (II), we start from the initial state:

$$
\rho = \frac{e^{-\beta_L(\mathcal{H}_L - \mu_L \mathcal{N}_L)}}{Z_L} \otimes |0\rangle \langle 0| \otimes \frac{e^{-\beta_R(\mathcal{H}_R - \mu_R \mathcal{N}_R)}}{Z_R}, \tag{56}
$$

where $\mathcal{N}_{L,R}$ are the number operators in the baths, $Z_x = \operatorname{Tr}\left(e^{-\beta_x(\mathcal{H}_x - \mu_x \mathcal{N}_x)}\right)$, $x = L, R$, the partition functions of the baths and $|0\rangle\langle 0|$ refers to the wire being initially completely empty. With this choice of the initial state, we can compute all the $t = 0$ correlations required in Eq. (54).

The eigenvalues and eigenfunctions of the matrix $\mathcal{Z}$ defined in the previous section, corresponding to the Hamiltonian Eq.(55), can be easily computed numerically for chains of finite length N_S. For our numerical example we take $N = 2$, $N_b = 100$, and use Eq. (54) in the previous section to calculate the time evolution, at any finite time, of the currents $J_L(t) = -2V_L\mathrm{Im}[\langle a_1^\dagger(t)b_1^L(t)\rangle]$, $J_R(t) = -2V_R\mathrm{Im}[\langle a_N^\dagger(t)b_1^R(t)\rangle]$ at the two boundaries and the densities $N_1(t) = \langle a_1^\dagger(t)a_1(t)\rangle$, $N_2(t) = \langle a_2^\dagger(t)a_2(t)\rangle$.
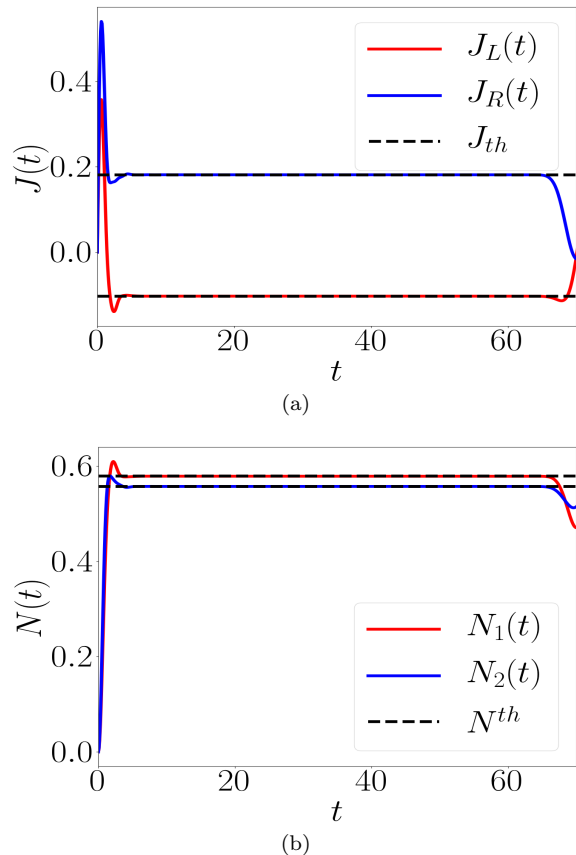

(a)

(b)

FIG. 1. Comparison of numerical time-evolution and analytical steady state results: Parameter values — $N = 2$, $N_b = 100$, $\mu_R = 1$, $\beta_R = 10$, $\mu_L = 0$, $\beta_L = 0$, $V_L = V_R = \eta_s = 1$, $\eta_b = 1.5$ and $\Delta = 0.40$. (a) Comparison of the numerically calculated current at the left, $J_L(t)$, and the right, $J_R(t)$, end of the wire with the corresponding value, J_{th}, given by the expression in Eq. (39). (b) Comparison of the numerically calculated densities, $N_1(t) = \langle a_1^\dagger(t)a_1(t)\rangle$ and $N_2(t) = \langle a_2^\dagger(t)a_2(t)\rangle$, on the two sites of the wire with the corresponding value, N_{th}, given by the expression in Eq. (43). The initial oscillations seen in the plots correspond to the transient phase, while the behaviour near $t = 60$ is due to the finite size of the baths. In the intermediate region we see perfect agreement between the numerical solution and the steady state value.

The general analytic expressions for the steady state properties of the wire are in terms of the two Green's functions $G_1^+(\omega)$ and $G_2^+(\omega)$ defined in Eq. (34) and Eq. (35) respectively. For the Hamiltonian given in Eq. (55), the various matrices involved in them take sim-

pler forms and one finds[23]:

$$K_{ij} = \Delta(\delta_{i,j+1} - \delta_{i,j-1}), \tag{57}$$

$$[\Sigma_L^+(\omega)]_{ij} = V_L^2 g(\omega)\delta_{i1}\delta_{j1}, \tag{58}$$

$$[\Gamma_L(\omega)]_{ij} = V_L^2 \,\mathrm{Im}\{g(\omega)\}\delta_{i1}\delta_{j1}, \tag{59}$$

$$[\Sigma_R^+(\omega)]_{ij} = V_R^2 g(\omega)\delta_{iN}\delta_{jN}, \tag{60}$$

$$[\Gamma_R(\omega)]_{ij} = V_R^2 \,\mathrm{Im}\{g(\omega)\}\delta_{iN}\delta_{jN}, \tag{61}$$

$$[\Pi(\omega)]_{ij} = \omega\delta_{ij} + \eta_s(\delta_{i,j+1} + \delta_{i,j-1}),$$
$$- V_L^2 g(\omega)\delta_{i1}\delta_{j1} - V_R^2 g(\omega)\delta_{iN}\delta_{jN}, \tag{62}$$

where $g(\omega) = [g_L^+(\omega)]_{11}$. Since $g_L^+(\omega)$ is the inverse of a tri-diagonal matrix, it can be shown that[23]

$$g(\omega) = \begin{cases} \frac{1}{\eta_b}\left(\frac{\omega}{2\eta_b} - \sqrt{\frac{\omega^2}{4\eta_b^2} - 1}\right), & \text{if } \omega > 2\eta_b \\ \frac{1}{\eta_b}\left(\frac{\omega}{2\eta_b} + \sqrt{\frac{\omega^2}{4\eta_b^2} - 1}\right), & \text{if } \omega < -2\eta_b \\ \frac{1}{\eta_b}\left(\frac{\omega}{2\eta_b} + i\sqrt{1 - \frac{\omega^2}{4\eta_b^2}}\right), & \text{if } |\omega| < 2\eta_b. \end{cases} \tag{63}$$

Using Eqs. (57-63) we can compute the steady state value of the current and densities by direct substitution of these expressions in Eq. (39) and Eq. (43). The integrations over ω in the resulting expressions are carried out numerically. In Fig. (1) we show the comparison between the values for the steady state current and densities obtained from Eqs. (39,43) with the corresponding values obtained from the direct time evolution.

In general we find that, for the parameter regimes over which there exists a steady state, Eq. (39) gives the value of the steady state current. We also verified that this expression reproduces the results given in Ref. [20]. As discussed in the end of Sec. (III), the non-vanishing of I_{ij} in fact indicates the presence of bound states which leads to the break-down of the NESS assumption. In Figs. (2a,2b) we show the full energy spectrum of the system for the parameter values $N = 2$, $N_b = 100$, $V^L = V^R = \eta_s = 1$, $\eta_b = 2.5$ and for two values of Δ. We see the appearance of a discrete energy level, indicating a bound state, for the parameter value $\Delta = 5$. In Fig. (3a) we show the variation, with Δ, of the quantity $\sum_{i,j}|I_{ij}|^2$ for different parameter regimes of the Hamiltonian in Eq. (55) with $N = 2$. We see that the bound state contribution, for any fixed η_b, only kicks in after some critical value of Δ. In Fig. (3b) we show the variation of the energy gap, between the bound state level and the band edge, over the same parameter regimes as in Fig. (3a). For any fixed η_b, we see that the bound state appears at the same value of Δ as that where I_{ij} in Fig. (3a) becomes non-vanishing.

VI. DISCUSSION

In conclusion, we considered transport in a wire that is modelled by a spinless superconductor with a mean-field pairing form for the interaction term, so that it is effectively described by a general quadratic Hamiltonian. We
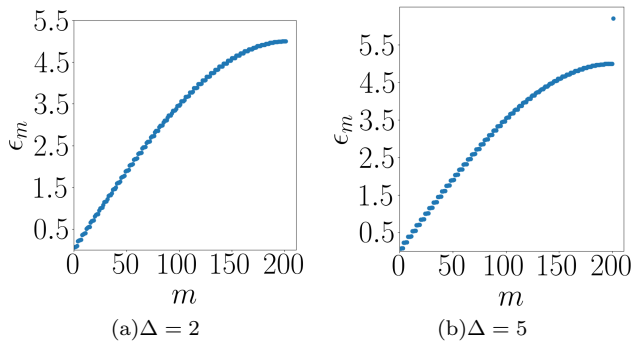
FIG. 2. Spectrum of the entire system at parameter values $N = 2$, $N_b = 100$, $V^L = V^R = \eta_s = 1$ and $\eta_b = 2.5$ for two values of Δ. In (a) we do not see any discrete energy level while in (b) a discrete energy level outside the main band can be seen. As discussed in the text, the non-existence of a steady state, indicated in a non-vanishing I_{ij}, is related to the existence of the discrete level which corresponds to a bound state (see Fig. (3)).
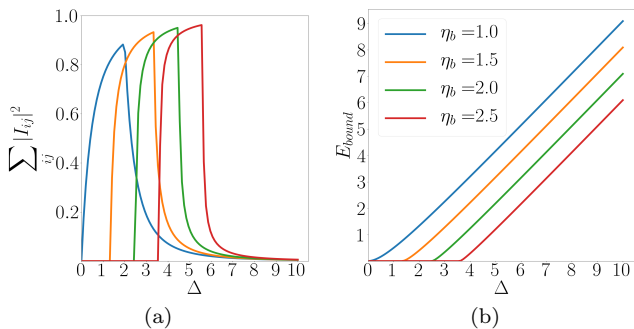

FIG. 3. (a) The variation of $\sum_{ij} |I_{ij}|^2$ over different parameters of the Hamiltonian in Eq. (55) with $\eta_s = V_L = V_R = 1$ and $N = 2$. Physically this quantity should identically vanish. We see that this happens only for for certain parameter regimes of the Hamiltonian. In (b) we verify that the non-zero values are associated to the presence of high energy bound states in the spectrum of the full system seen in Fig. (2). This plot shows the gap between the bound state energy, E_{bound}, and the edge of the band for the same parameters as in (a). We see that the value of Δ at which the bound state appears is exactly at the same where the corresponding curves in (a) start taking non-zero values.

investigated transport in the wire for the so-called N-S-N geometry where the superconductor is placed between normal leads. Thus, in our set-up, the wire is attached to free electron baths at different temperatures and chemical potentials and we investigated particle transport, using the open system framework of quantum Langevin equations (QLE) and nonequilibrium Green's function (NEGF).

Our main results are the exact analytic expressions for the current and other two-point correlations in the nonequilibrium steady state. These have the same structure as NEGF expressions for free electrons, but now involve two sets of Green's functions. To derive these expressions we have to assume the existence of a nonequilibrium steady state and this is related to the existence of bound states (discrete energy levels) in the spectrum of the entire coupled system of the superconducting wire and the baths (non-interacting normal electrons). The role of bound states on the existence of steady states is known for normal systems[23,27,28] and has recently been investigated for the case of superconductors in Ref. [21]. In the present work we examined this issue for the one-dimensional Kitaev chain. By performing an exact numerical diagonalization of the full quadratic Hamiltonian of wire and baths, we computed the time evolution of the current and local densities, starting from the same initial density matrix as used in the steady state calculations. We then showed that the results from this approach agree perfectly with the analytic expressions, for the case where there are no bound states. On the other hand, the presence of bound states leads to non-physical results from the analytic expressions, such as non-vanishing of the expectation value of fermionic anti-commutators. These bound states are high energy excited states and distinct from the Majorana bound states (MBS) of the Kitaev chain. A very interesting question that requires further investigation is as to what happens to the MBS in a long Kitaev wire on being connected to leads, especially for the case of strong coupling between the wire and leads.

In the present work we have not imposed the self-consistency condition for the superconducting pairing terms and we saw that this leads to the non-conservation of particle number in the wire. Physically this corresponds to the situation of proximity-induced superconductivity, where the wire is placed on a superconducting substrate that is grounded and hence serves as a sink (or source) of electrons. Another interesting situation would be one where one is actually looking at transport through a superconductor and the self-consistency condition has to be introduced. This appears to be quite non-trivial and our results, which provide analytic expressions for all two-point correlations in the nonequilibrium steady state, provides a good starting point to study this problem.

[1] A. Y. Kitaev, Unpaired majorana fermions in quantum wires, Physics-Uspekhi **44**, 131 (2001).

[2] L. Fu and C. L. Kane, Superconducting proximity effect and majorana fermions at the surface of a topological insulator, Physical review letters **100**, 096407 (2008).

[3] J. D. Sau, R. M. Lutchyn, S. Tewari, and S. D. Sarma, Generic new platform for topological quantum computation using semiconductor heterostructures, Physical review letters **104**, 040502 (2010).

[4] R. M. Lutchyn, J. D. Sau, and S. D. Sarma, Majorana fermions and a topological phase transition in semiconductor-superconductor heterostructures, Physical review letters **105**, 077001 (2010).

[5] Y. Oreg, G. Refael, and F. von Oppen, Helical liquids and majorana bound states in quantum wires, Physical review letters **105**, 177002 (2010).

[6] J. D. Sau, S. Tewari, R. M. Lutchyn, T. D. Stanescu, and S. D. Sarma, Non-abelian quantum order in spin-orbit-coupled semiconductors: Search for topological majorana particles in solid-state systems, Physical Review B **82**, 214509 (2010).

[7] V. Mourik, K. Zuo, S. M. Frolov, and S. Plissard, Ep a. m. bakkers, and lp kouwenhoven, Science **336**, 1003 (2012).

[8] A. Das, Y. Ronen, Y. Most, Y. Oreg, M. Heiblum, and H. Shtrikman, Zero-bias peaks and splitting in an al–inas nanowire topological superconductor as a signature of majorana fermions, Nature Physics **8**, 887 (2012).

[9] M. Deng, C. Yu, G. Huang, M. Larsson, P. Caroff, and H. Xu, Anomalous zero-bias conductance peak in a nb–insb nanowire–nb hybrid device, Nano letters **12**, 6414 (2012).

[10] L. P. Rokhinson, X. Liu, and J. K. Furdyna, The fractional ac josephson effect in a semiconductor–superconductor nanowire as a signature of majorana particles, Nature Physics **8**, 795 (2012).

[11] A. Finck, D. J. Van Harlingen, P. Mohseni, K. Jung, and X. Li, Anomalous modulation of a zero-bias peak in a hybrid nanowire-superconductor device, Physical review letters **110**, 126406 (2013).

[12] H. Churchill, V. Fatemi, K. Grove-Rasmussen, M. Deng, P. Caroff, H. Xu, and C. M. Marcus, Superconductor-nanowire devices from tunneling to the multichannel regime: Zero-bias oscillations and magnetoconductance crossover, Physical Review B **87**, 241401 (2013).

[13] A. M. Lobos and S. D. Sarma, Tunneling transport in NSN majorana junctions across the topological quantum phase transition, New Journal of Physics **17**, 065010 (2015).

[14] R. Shankar, Topological insulators–a review, arXiv preprint arXiv:1804.06471 (2018).

[15] G. E. Blonder, M. Tinkham, and T. M. Klapwijk, Transition from metallic to tunneling regimes in superconducting microconstrictions: Excess current, charge imbalance, and supercurrent conversion, Phys. Rev. B **25**, 4515 (1982).

[16] M. Thakurathi, O. Deb, and D. Sen, Majorana modes and transport across junctions of superconductors and normal metals, Journal of Physics: Condensed Matter **27**, 275702 (2015).

[17] A. Maiellaro, F. Romeo, C. A. Perroni, V. Cataudella, and R. Citro, Unveiling signatures of topological phases in open kitaev chains and ladders, Nanomaterials **9**, 894 (2019).

[18] R. Doornenbal, G. Skantzaris, and H. Stoof, Conductance of a finite kitaev chain, Physical Review B **91**, 045419 (2015).

[19] A. Komnik, Transport properties of hybrid topological superconductor devices in contact with an environment, Physical Review B **93**, 125117 (2016).

[20] D. Roy, C. Bolech, and N. Shah, Majorana fermions in a topological superconducting wire out of equilibrium: Exact microscopic transport analysis of a p-wave open chain coupled to normal leads, Physical Review B **86**, 094503 (2012).

[21] N. Bondyopadhaya and D. Roy, Dynamics of hybrid junctions of majorana wires, Physical Review B **99** (2019).

[22] G. Ford, M. Kac, and P. Mazur, Statistical mechanics of assemblies of coupled oscillators, Journal of Mathematical Physics **6**, 504 (1965).

[23] A. Dhar and D. Sen, Nonequilibrium greens function formalism and the problem of bound states, Physical Review B **73**, 085119 (2006).

[24] A. Dhar and D. Roy, Heat transport in harmonic lattices, Journal of Statistical Physics **125**, 801 (2006).

[25] A. R. Akhmerov, J. P. Dahlhaus, F. Hassler, M. Wimmer, and C. W. J. Beenakker, Quantized conductance at the majorana phase transition in a disordered superconducting wire, Phys. Rev. Lett. **106**, 057001 (2011).

[26] J.-P. Blaizot and G. Ripka, *Quantum theory of finite systems*, Vol. 3 (MIT press Cambridge, MA, 1986).

[27] G. Stefanucci, Bound states in ab initio approaches to quantum transport: A time-dependent formulation, Physical Review B **75**, 195115 (2007).

[28] É. Jussiau, M. Hasegawa, and R. S. Whitney, Signature of the transition to a bound state in thermoelectric quantum transport, Physical Review B **100**, 115411 (2019).

Appendix A: Derivation of the current expression

We present the derivation of the expression for the current in Eq. (39) here. We start by substituting Eq. (38) in Eq. (37) we get,

$$
J_L = 2\text{Im}\Big\{ \int d\omega d\omega' e^{i(\omega-\omega')t} \\
\langle c_m^\dagger(\omega)\{\eta_m^L(\omega') + [\Sigma_L^+(\omega')]_{ml}\tilde{c}_l(\omega')\}\rangle \Big\}
\tag{A1}
$$

Using Eq. (33) in the above expression we have,

$$
\Big\langle c_m^\dagger(\omega)\{\eta_m^L(\omega') + [\Sigma_L^+(\omega')]_{ml}\tilde{c}_l(\omega')\}\Big\rangle \\
= T_1 + T_2 + T_3 + T_4 + T_5
\tag{A2}
$$

where,

$$T_1 = \int_{-\infty}^{\infty}\int_{-\infty}^{\infty} d\omega d\omega' e^{i(\omega-\omega')t}[G_1^-(\omega)]_{km}\left\langle \eta_k^{L\dagger}(\omega)\eta_m^L(\omega')\right\rangle = \int_{-\infty}^{\infty} d\omega\,\mathrm{Tr}\big[G_1^-(\omega)\Gamma_L(\omega)\big]f_L(\omega)$$

$$T_2 = \int_{-\infty}^{\infty}\int_{-\infty}^{\infty} d\omega d\omega' e^{i(\omega-\omega')t}[G_1^-(\omega)]_{km}[\Sigma_L^+(\omega')]_{ml}[G_1^+(\omega')]_{lk'}\left\langle \eta_k^{L\dagger}(\omega)\eta_{k'}^L(\omega')\right\rangle$$

$$= \int_{-\infty}^{\infty} d\omega\,\mathrm{Tr}\big[G_1^-(\omega)\Sigma_L^+(\omega)G_1^+(\omega)\Gamma_L(\omega)\big]f_L(\omega) \tag{A3}$$

$$T_3 = \int_{-\infty}^{\infty}\int_{-\infty}^{\infty} d\omega d\omega' e^{i(\omega-\omega')t}[G_1^-(\omega)]_{km}[\Sigma_L^+(\omega')]_{ml}[G_1^+(\omega')]_{lk'}\left\langle \eta_k^{R\dagger}(\omega)\eta_{k'}^R(\omega')\right\rangle$$

$$= \int_{-\infty}^{\infty} d\omega\,\mathrm{Tr}\big[G_1^-(\omega)\Sigma_L^+(\omega)G_1^+(\omega)\Gamma_R(\omega)\big]f_R(\omega) \tag{A4}$$

$$T_4 = \int_{-\infty}^{\infty}\int_{-\infty}^{\infty} d\omega d\omega' e^{i(\omega-\omega')t}[G_2^-(\omega)]_{km}[\Sigma_L^+(\omega')]_{ml}[G_2^+(\omega')]_{lk'}\left\langle \eta_k^L(-\omega)\eta_{k'}^{L\dagger}(-\omega')\right\rangle$$

$$= \int_{-\infty}^{\infty} d\omega\,\mathrm{Tr}\big[G_2^-(\omega)\Sigma_L^+(\omega)G_2^+(\omega)\Gamma_L^T(-\omega)\big](1-f_L(-\omega)) \tag{A5}$$

$$T_5 = \int_{-\infty}^{\infty}\int_{-\infty}^{\infty} d\omega d\omega' e^{i(\omega-\omega')t}[G_2^-(\omega)]_{km}[\Sigma_L^+(\omega')]_{ml}[G_2^+(\omega')]_{lk'}\left\langle \eta_k^R(-\omega)\eta_{k'}^{R\dagger}(-\omega')\right\rangle$$

$$= \int_{-\infty}^{\infty} d\omega\,\mathrm{Tr}\big[G_2^-(\omega)\Sigma_L^+(\omega)G_2^+(\omega)\Gamma_R^T(-\omega)\big](1-f_R(-\omega)) \tag{A6}$$

The imaginary parts of T_1, T_2, T_3, T_4 and T_5 can be shown to be the following,

$$\mathrm{Im}\{T_1\} = \int_{-\infty}^{\infty} d\omega\,\mathrm{Tr}\big[\mathrm{Im}\{G_1^-(\omega)\}\Gamma_L(\omega)\big]f_L(\omega) \tag{A7}$$

$$\frac{-1}{\pi}\mathrm{Im}\{T_2\} = \tag{A8}$$

$$\int_{-\infty}^{\infty} d\omega\,\mathrm{Tr}\big[G_1^-(\omega)\Gamma_L(\omega)G_1^+(\omega)\Gamma_L(\omega)\big]f_L(\omega)$$

$$\frac{-1}{\pi}\mathrm{Im}\{T_3\} = \tag{A9}$$

$$\int_{-\infty}^{\infty} d\omega\,\mathrm{Tr}\big[G_1^-(\omega)\Gamma_L(\omega)G_1^+(\omega)\Gamma_R(\omega)\big]f_R(\omega)$$

$$\frac{1}{\pi}\mathrm{Im}\{T_4\} = \tag{A10}$$

$$\int_{-\infty}^{\infty} d\omega\,\mathrm{Tr}\big[G_2^-(\omega)\Gamma_L(\omega)G_2^+(\omega)\Gamma_L^T(-\omega)\big](f_L(-\omega)-1)$$

$$\frac{1}{\pi}\mathrm{Im}\{T_5\} = \tag{A11}$$

$$\int_{-\infty}^{\infty} d\omega\,\mathrm{Tr}\big[G_2^-(\omega)\Gamma_L(\omega)G_2^+(\omega)\Gamma_R^T(-\omega)\big](f_R(-\omega)-1)$$

It is fairly straightforward to show that,

$$\mathrm{Im}\{G_1^-(\omega)\} = \pi\big[G_1^+(\omega)(\Gamma_L(\omega)+\Gamma_R(\omega))G_1^-(\omega)$$
$$+ G_2^+(\omega)(\Gamma_L^T(-\omega)+\Gamma_R^T(-\omega))G_2^-(\omega)\big]$$

Substituting this result in Eq. (A7) and adding up the imaginary parts of the terms T_1, T_2, T_3, T_4 and T_5, we obtain the required expression for the current entering the wire from the left reservoir to be

$$\frac{J_L}{2\pi} =$$
$$\int_{-\infty}^{\infty} d\omega\bigg(\mathrm{Tr}\big[G_1^+(\omega)\Gamma_R(\omega)G_1^-(\omega)\Gamma_L(\omega)\big](f_L(\omega)-f_R(\omega))$$
$$+ \mathrm{Tr}\big[G_2^+(\omega)\Gamma_R^T(-\omega)G_2^-(\omega)\Gamma_L(\omega)\big](f_R(-\omega)+f_L(\omega)-1)$$
$$+ \mathrm{Tr}\big[G_2^+(\omega)\Gamma_L^T(-\omega)G_2^-(\omega)\Gamma_L(\omega)\big](f_L(-\omega)+f_L(\omega)-1)\bigg)$$

The current from the right reservoir into the wire, J_R can be obtained with similar algebra and is given by,

$$\frac{J_R}{2\pi} =$$
$$\int_{-\infty}^{\infty} d\omega\bigg(\mathrm{Tr}\big[G_1^+(\omega)\Gamma_L(\omega)G_1^-(\omega)\Gamma_R(\omega)\big](f_R(\omega)-f_L(\omega))$$
$$+ \mathrm{Tr}\big[G_2^+(\omega)\Gamma_L^T(-\omega)G_2^-(\omega)\Gamma_R(\omega)\big](f_L(-\omega)+f_R(\omega)-1)$$
$$+ \mathrm{Tr}\big[G_2^+(\omega)\Gamma_R^T(-\omega)G_2^-(\omega)\Gamma_R(\omega)\big](f_R(-\omega)+f_R(\omega)-1)\bigg)$$